InSAR GEOMETRY AND BASIC OPERATIONS

Andon Dimitrov Lazarov
Burgas Free University

InSAR ГЕОМЕТРИЯ И БАЗОВИ ОПЕРАЦИИ

Андон Димитров Лазаров

Abstract: *In the present work based on geometrical interpretation of Inverse Synthetic Aperture Radar (InSAR) scenario, main parameters, characteristics and operations over InSAR data are defined. SAR interferogram and interferometric phase SAR equations are derived and procedure of interferogram flattening is given. The procedures of terrain motion evaluation and differential interferogram generation are presented. Basic operations including rectification of the elevation map, co-registration, and coherence evaluation, and phase unwrapping are discussed. Numerical experiment is carried out to verify geometrical interpretation of the interferogam generation and main operation performance.*

Key words: InSAR geometry, InSAR equations.

1. Introduction

Synthetic Aperture Radar (SAR) is a coherent active microwave imaging sensor. Backscattered information of a target is recorded as a 2-D complex signal with amplitude and phase information from which SAR complex valued image with amplitude and phase is extracted. Interferometric SAR (In-SAR) technique makes use of phase difference information extracted from two complex valued SAR images acquired from different orbit positions. This information is useful in measuring several geophysical quantities such as topography, slope, deformation (volcanoes, earthquakes, and ice fields), glacier studies, vegetation growth etc. With increase in number of SAR sensors in orbit, In-SAR technique is rapidly gaining importance in remote sensing of planet earth. Also, SAR system is able to provide data for all weather as well as day and night. This way it guarantees global coverage of the Earth.
SAR Interferometry was first used for topographic mapping by Graham in 1974 *(Graham, L.C., 1974).* The first practical results were obtained by Zebker and Goldstein using side looking airborne radar in 1986 (*Zebker, H.A., Goldstein, R.M., 1986*). Studies on interferometric SAR (InSAR) were extended after the launch of ERS-1 and ERS-2 satellites, which can provide interferometric data acquired only one day apart. The number of scientific research on InSAR technology has also exploded since the launch of new satellites such as ENVISAT.
In order to obtain SAR Interferometric data, two spatially separated antennas the physical separation of which is called the interferometric baseline are mounted on a single platform or one antenna is mounted on a satellite and data sets are acquired by passing the same area twice. In the latter case, the interferometric baseline is formed by relating radar signals on repeat passes over the target area. This approach is called *repeat-pass interferometry*.

The main goal of the present work is to define the geometry InSAR scenario and based on its geometrical interpretation to define main parameters, characteristics and operations over InSAR data to be defined.
The rest of the paper is organized as follows. In Section 2 InSAR geometry and basic geometric and interferometric phase equations are described, and terrain motion evaluation is considered. In Section 3 basic InSAR operations for interferograms generation are defined. In Section 4 numerical experimental results are considered. In Section 5 conclusions are made.

2. InSAR Geometry and Basic Equations

2.1. InSAR Geometrical Equations.

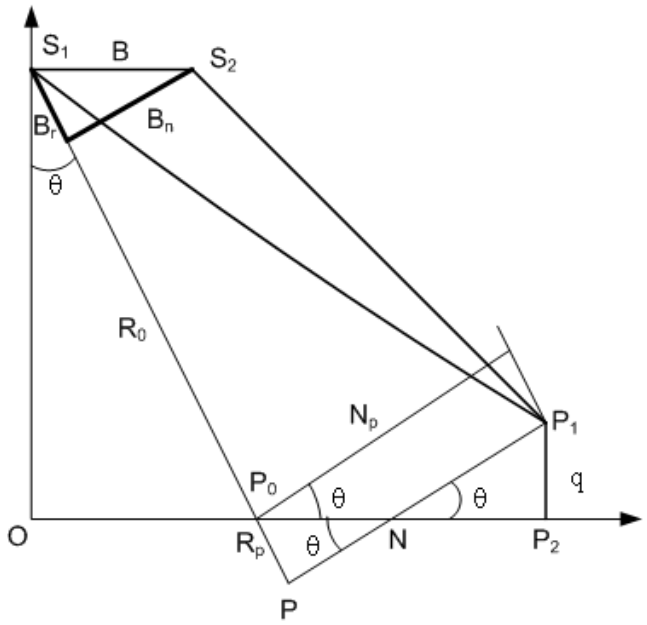

Fig. 1. InSAR geometry: B - the base line; B_r - the radial base line; B_n - the normal base line.

Consider two positions S_1 and S_2 of the satellite ENVISAT with ASAR mounted on it [1]. In the position of the satellite S_1 the following geometrical relations hold.
$R_0 = S_1P_0$ - is the distance from the position of the satellite S_1 to the reference point P_0, lying on the zero level, R_0 - the reference line of sight, $R_p = P_0P$ - the displacement of the phase front of the flat electromagnetic wave along the line of sight from the reference point P_0 to the point P_1, lying in nearest resolution cell at height $q = P_1P_2$ from the zero level. From geometrical relations in the triangle S_1PP_1 the slant range distance $R_1 = S_1P_1$ can be written as

$$R_1 = S_1P_1 = \sqrt{(R_0 + R_p)^2 + N_p^2} \quad (3)$$

where $N_p = PP_1$ is the vertical displacement of the point P_1 with respect to the reference line of sight and R_p is the displacement of the point P_1 along the reference line of sight with respect to reference point P_0 (Fig. 1).

From triangles R_pPN and NP_1P_2, and the geometrical relation $N_p = PN + NP_1$ the following equation can be written

(4) $$N_p = \frac{R_p}{\tan\theta} + \frac{q}{\sin\theta}.$$

In the position of the satellite S_2 taking into account negative displacements B_r, radial base line, along the reference line, and B_n, normal base line, normal to the reference line, the distance $R_2 = S_2P_1$ can be written as

(5) $$R_2 = S_2P_1 = \sqrt{(R_0 + R_p - B_r)^2 + (N_p - B_n)^2}.$$

Since the distance B_n measured on the normal to the reference line between the two SAR sensors is much smaller than the SAR-target distance, R_0, the range difference $\Delta R = (S_2P_1 - S_1P_1)$ can be expressed as

(6) $$\Delta R = \frac{B_nN_p}{R_0}.$$

Taking into account (4) the distance variation to the point P_1 can be written as

(7) $$\Delta R = \frac{B_n}{R_0}\left(\frac{R_p}{\tan\theta} + \frac{q}{\sin\theta}\right).$$

2.2. Iinterferometric SAR phase equations

The phase difference corresponding to the distance variation ΔR is proportional to the travel path difference $2\Delta R$ (the factor 2 accounts for the two ways travel path from S_1 and S_2 to P_1), i.e.

(8) $$\Phi = k(2\Delta R),$$

where $k = \frac{2\pi}{\lambda}$ is the wave number; λ is the wavelength.

Thus, based on (5) and (6) the phase difference called an interferomegtric phase can be expressed as

(9) $$\Phi = \frac{4\pi}{\lambda}.\frac{B_n}{R_0}\left(\frac{R_p}{\tan\theta} + \frac{q}{\sin\theta}\right).$$

The phase difference is divided into to two components

$\Phi_1 = \frac{4\pi}{\lambda}.\frac{B_n}{R_0}\left(\frac{R_p}{\tan\theta}\right)$- phase variation proportional to the slant range displacement R_p of point targets P_1 and P_0.

$\Phi_2 = \frac{4\pi}{\lambda}.\frac{B_n}{R_0}\left(\frac{q}{\sin\theta}\right)$ - phase variation proportional to the altitude difference q between point targets P_1 and P_0, referred to a horizontal reference plane.

Multiplication of the complex interferogram with complex conjugated phase term $\exp(-j\Phi_1)$ is called interferogram flattening. It generates a phase map proportional to the relative terrain altitude.

The change of the phase with elevation of the target point is given by the derivative

(10) $$\frac{d\Phi}{dq} = \frac{4\pi.B_n}{\lambda R_0 \sin\theta}$$

This relation describes the height sensitivity of interferometric measurements, which may also be described by the height or altitude of ambiguity.

The altitude of ambiguity H_a is defined as the altitude difference that generates an interferometric phase change of 2π after interferogram flattening. The altitude of ambiguity is proportional to the wavelength, reference slant range distance and sinus of look angle θ, and inversely proportional to the perpendicular baseline B_n:

(11) $$H_a = \frac{\lambda R_0 \sin\theta}{2B_n}$$

According to this relation long baselines would be preferable to derive accurate elevation data from InSAR measurements, but there are theoretical and practical limits. Above a certain baseline (the critical baseline) the spectral shift between the two SAR images exceeds the system bandwidth, and interferograms cannot be formed.

2.3. Terrain motion measurement: Differential Interferometry

In case point scatterers on the ground slightly change their relative position in time interval between two SAR acquisitions (in the event of subsidence, landslide, earthquake, etc.) an additive phase term independent of the baseline, proportional to the projection d of the displacement on the slant range direction, i.e.

(12) $$\Phi_3 = -\frac{4\pi}{\lambda}d\ .$$

Thus, after interferogram flattening the resulting interferometric phase contains altitude and motion contributions, i.e.

(13) $$\hat{\Phi} = \Phi_2 + \Phi_3 = \frac{4\pi}{\lambda}.\frac{B_n}{R_0}\left(\frac{q}{\sin\theta}\right) - \frac{4\pi}{\lambda}d\ .$$

In order to reveal the motion contribution term a differential InSAR technique is applied. Consider the case of single interferometric pair (master and slave) acquired by non-zero baseline and available DEM. The processing steps are:

- DEM must be converted from geographic to SAR coordinates and the elevation must be converted into interferometric phases (interferometric fringes). The baseline should be the same as used for the interferometric pair.
- Synthetic interferometric phases should be subtracted from those of the available interferometric pair. This operation can be conveniently done in the complex domain by multiplying the actual interferogram by the complex conjugate of the synthetic one.

Consider the case with three SAR images and no terrain motion between two of them, one image should be selected as a common master. Two interferograms are then formed: the two slave images are co-registered to the common master. The shortest temporal difference (to gain

coherence and avoid terrain motion) and a medium/high baseline (to gain elevation accuracy) should be selected for the first interferometric pair. The second pair should have a larger temporal difference (it should contain the terrain motion) and a short baseline. The processing steps include:
- The first interferogram should be unwrapped and scaled by the ratio of the two baselines.
- Its phase should be wrapped again and subtracted from that of the second interferogram (generally done in the complex domain).
If the baselines of the two interferometric pairs are in an integer ratio, unwrapping can be avoided. The phases of one interferogram can be directly scaled by the integer ratio between baselines and subtracted from the phases of the other interferogram.

3. Basic InSAR operations

3.1. Rectification of the elevation map

Due to the low off-nadir angle of the satellites (23° at mid-swath), significant layover effects are often observed in areas with rough topography. When the surface slope approaches the incidence angle, the ground-range sampling step becomes wider and wider, so that a single measurement (often unreliable due to geometric decorrelation) characterises many output pixels in geographical coordinates. For that reason, ascending and descending data fusion is essential for slope coverage in SAR interferometry: areas affected by foreshortening and layover in one mode are well covered (if not in shadow) in the other one. The quality of such a combination is strongly dependent on the accuracy of the ortho-rectification step.
The SAR image is acquired in 2-D coordinates: slant range and azimuth. In order to rectify image, i.e. to put it in 2-D coordinated ground range and azimuth the horizontal displacement P_0P_2 of each point target with respect to the initial point P_0 on the reference line of sight have to be defined. It is a sum of two components: the first is the horizontal displacement in case the target point lies on flat terrain, the second caused by a non-zero elevation drop of the target point, i.e.

(14) $$P_0P_2 = P_0N + NP_2,$$

where $P_0N = \frac{R_p}{\sin\theta}$, $NP_2 = \frac{q}{\tan\theta}$.

Since the position of the points depends on its elevation, the correspondence between ground range and slant range is quite irregular. In fact, the well known foreshortening effect causes a compression of the areas with ascending slope and a spread of the descending areas. As a consequence the ground difference, corresponding to a constant slant range displacement, will be much larger in the case of ascending slopes. Furthermore, when layover effects occur, several areas of the earth's surface can disappear from the SAR image [1].
In a ground range reference system the obtained elevation map will have a quite uneven sampling interval. Thus to obtain a regular sampled map the elevation values must be interpolated. For our purposes a linear interpolation is quite adequate. In fact, in flat or descending areas the interpolating points are fairly close, whereas with an ascending slope the foreshortening effect produces such a large slant range compression that the interpolating points lie much further away and no interpolator would operate correctly [1].

3.2. Co-registration

The co-registration is a fundamental step in interferogram generation and consists in the definition of co-registering coefficients. It ensures that each ground target point contributes to

the same (range, azimuth) pixel in both the master and the slave image. Proper space alignment between the two images should be performed on a pixel by pixel basis, with accuracy of the order of one tenth of the resolution, or better.

Co-registration depends on the (local) topography. However the impact of the elevation is almost negligible in most cases. Therefore, the co-registration map can be provided as a smooth polynomial that approximates the pixel-to-pixel shift with the assumption of targets lying on the ellipsoidal Earth surface. In satellite-borne Synthetic Aperture Radars such as ERS and Envisat ASAR, the sensor velocity and attitudes are so stable that the master-slave displacement on the frame (100 × 100 km) can be well approximated by the following polynomial [1]:

$$r^S = a\left(r^M\right)^2 + br^M + c(as)^M + d \tag{15}$$

$$(as)^S = e\left(r^M\right)^2 + fr^M + g(as)^M + h\,, \tag{16}$$

where r^M, $(as)^M$ are range and azimuth coordinates of the pixels on the master SAR image; r^S, $(as)^S$ are range and azimuth coordinates of the pixels on the slave SAR image.

Co-registration coefficients can be computed by least mean square regression based on a regular grid of points displaced over the whole frame of the SAR image.

3.3. Coherence

A precondition for calculating an interferogram is that the phase within the borders of the pixel is preserved, that means the SAR return in the two complex images is correlated). The complex coherence c quantifies the phase relation between pixels in two SAR images

The coherence of co-registered SAR images is calculated as a modulus of the complex coefficient of coherence defined for a particular pixel of the master and slave images by expression

$$\dot{\gamma} = \frac{\sum_{a\in N}\sum_{r\in K} S_{ar}^M \left(S_{ar}^S\right)^*}{\left\{\sum_{a\in N}\sum_{r\in K} S_{ar}^M \left(SM_{ar}^M\right)^* \times \sum_{a\in N}\sum_{r\in K} S_{ar}^S \left(S_{ar}^S\right)^*\right\}^{\frac{1}{2}}} \tag{17}$$

where S_{ar}^M and S_{ar}^S are where are complex values of *ar*-th resolution element from master and slave images, *N* is the number of azimuth resolution elements and *K* is the number of range resolution elements in the particular pixel of the SAR image.

The coherence magnitude $\mathrm{mod}(\dot{\gamma})$ of the estimate (also called degree of coherence) is used to describe the phase relation.

3.4. Phase Unwrapping

Phase unwrapping is the process of recovering the absolute phase from the wrapped phase. This is, however, an ill-posed problem, if no further information is added. In fact, an assumption taken by most phase unwrapping algorithms is that the absolute value of phase differences between neighboring pixels is less than π, the so-called Itoh condition [11]. If this assumption is not violated, the absolute phase can be easily determined, up to a constant. Itoh condition might be violated if the true phase surface is discontinuous, or if only a noisy version of the wrapped phase is available. In either case, PU becomes a very difficult problem, to which much attention has been devoted [12, 13].

Phase Unwrapping Least-Squares Method

Phase unwrapping is the process of recovering the absolute phase from the wrapped phase. The main idea is to minimize the distance between the discrete gradient of unwrapped phase and the discrete gradient estimated from the value of the wrapped phase. Denote the measured (wrapped) phase value in (*i,j*)-th range-azimuth resolution element of the SAR image by $\psi_{i,j}$, modulo-2π and the true (the so called absolute value) sought after unwrapped phase value by φ_{ij}, on a discrete grid of points then

$$\psi_{i,j} = \varphi_{ij} + 2\pi k \tag{18}$$

where $k \in \mathbf{Z}$ is an integer number of wavelengths, $-\pi < \psi_{ij} > \pi$, $i = \overline{0, M-1}$, $j = \overline{0, N-1}$.

The following wrapped phase differences can be computed from the wrapped phase $\psi_{i,j}$

$$\nabla^x_{i,j} = W\left(\psi_{i+1,j} - \psi_{i,j}\right) \text{ for } i = \overline{0, M-2},\ j = \overline{0, N-1};$$

$$\nabla^x_{i,j} = 0 \text{ ,otherwise.}$$

(19)

$$\nabla^y_{i,j} = W\left(\psi_{i,j+1} - \psi_{i,j}\right) \text{ for } i = \overline{0, M-1},\ j = \overline{0, N-2};$$

$$\nabla^x_{i,j} = 0 \text{ , otherwise.}$$

where *W*(.) is the wrapping operator over a partial solution ϕ_{ij}, i.e. $W(\phi_{i,j}) = \phi_{i,j} + 2\pi k_{i,j}$

where $k_{i,j}$ is an integer chosen so that $W(\phi_{i,j}) \in (-\pi, \pi]$.

Assume that the phase differences of phases $\varphi_{i,j}$ of adjacent pixels are less than π in magnitude everywhere. The phase unwrapping problem reduces to minimization in least square sense of the discrete functional defined by the sum of differences between the partial derivatives of solution ϕ_{ij} and those defined by equations (18), i.e.

$$J = \sum_{i=0}^{M-2}\sum_{j=0}^{N-1}\left(\phi_{i+1,j} - \phi_{i,j} - \nabla^x_{i,j}\right)^2 + \sum_{i=0}^{M-1}\sum_{j=0}^{N-2}\left(\phi_{i,j-1} - \phi_{i,j} - \nabla^y_{i,j}\right)^2 . \tag{19}$$

The derivative $\frac{dJ}{d\varphi_{i.j}} = 0$ yields the discrete Poison equation

$$\left(\phi_{i+1,j} - 2\phi_{i,j} - \phi_{i-1,j}\right) + \left(\phi_{i,j+1} - 2\phi_{i,j} - \phi_{i,j-1}\right) = \left(\nabla^x_{i,j} - \nabla^x_{i-1,j}\right) + \left(\nabla^y_{i,j} - \nabla^y_{i,j-1}\right) \tag{20}$$

The equation (20) can be solved by multigrid method described in [14, 15].

4. Numerical experiment

Assume InSAR system comprising three satellites with initial space coordinates $x_0^1 = 0$ m; $y_0^1 = 200.10^3$; $z_0^1 = 200.10^3$ m; $x_0^2 = 0$ m.; $y_0^2 = 200{,}6.10^3$ m; $z_0^2 = 200.10^3$ m; and coordinates of vector-velocity of satellites: $v_x = 0$ m/s; $v_y = -600$ m/s; $v_z = 0$ m/s.

SAR cluster observes a surface (Fig. 2) depicted by equation

$$z_{ij} = 3(1-x_{ij})^2 \exp[-x_{ij}{}^2 - (y_{ij}+1)^2] - 10\left(\frac{x_{ij}}{5} - x_{ij}{}^3 - y_{ij}{}^5\right)\exp(-x_{ij}{}^2 - y_{ij}{}^2) -$$

$$-\frac{1}{3}\exp[-(x_{ij}+1)^2 - y_{ij}{}^2]$$

modified in a way negative values to be transformed in the range from 0 to 1, where $x_{ij} = i\Delta X$, $y_{ij} = j\Delta Y$, $i = \overline{1,I}$, $j = \overline{1,J}$, I = 128; J = 128; ΔX; ΔY - the spatial dimensions of the 2-D grid cell.

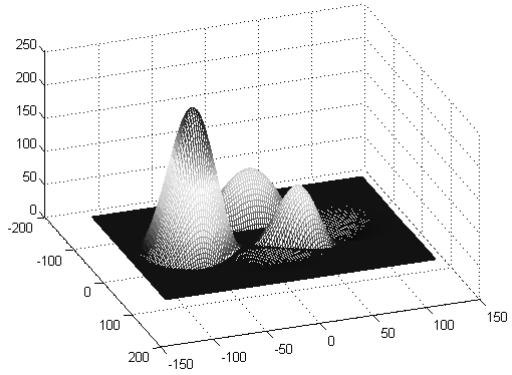

Fig. 2. Surface of observation.

Normalized amplitude of reflected signals from every pixel $a_{ij} = 0.01$. Dimensions of the resolution element (pixel) are $\Delta X = \Delta Y = 2$ m. Radara parameters: wavelength 0.1 m., carrier frequency 3.10^9 Hz, frequency bandwidth $\Delta F = 3{,}75.10^7$ Hz, pulse repetition period $T_p = 4{,}41.10^{-2}$ s, pulse duration $T = 5.10^{-6}$ s, sample time duration $\Delta T = 1{,}95.10^{-8}$ s, LFM samples 256. Emitted pulses are 256. Co-registration of two SAR images is carried out within high pixel accuracy. The wrapped SAR interferograms of the observation scene and reference plane (the surface on zero level) are presented in Fig.3, *a* and Fig. 3, *b*, respectively. It can be seen three areas with fringes depicting parts on the ground with different height, and two areas with law level of the surface (Fig.3, *a*).

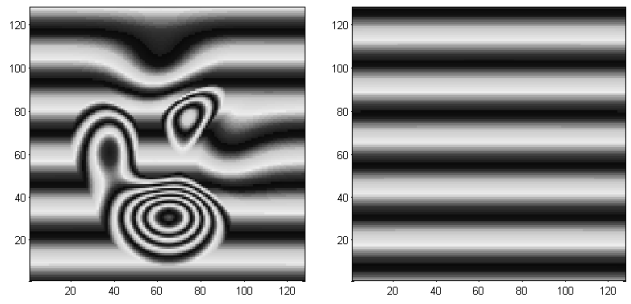

(*a*) (*b*)

Fig. 3. Wrapped interferogram of the SAR image (*a*); wrapped interferogram of base plane (zero surface) (*b*).

Matlab standard phase unwrapping procedure for phase relief extraction from the interferogram (Fig.3, *a*) is carried out. The result is illustrated in Fig. 5.

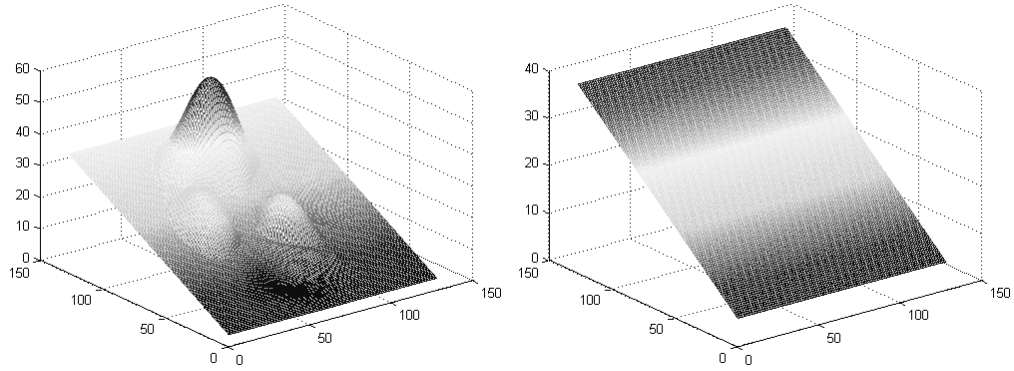

Fig. 4. Unwrapped interferogram of the scene. Fig. 5. Unwrapped interferogram of the base plane.

In order to flatten an unwrapped interferogram of the scene (Fig. 4) Matlab standard phase unwrapping procedure is also applied to a wrapped interferogram of the base plane (Fig. 3, *b*). The result is shown in Fig. 5. The flattening procedure consists in subtraction of unwrapped interferogram phases of both the scene and base plane. The result is presented in Fig. 6.

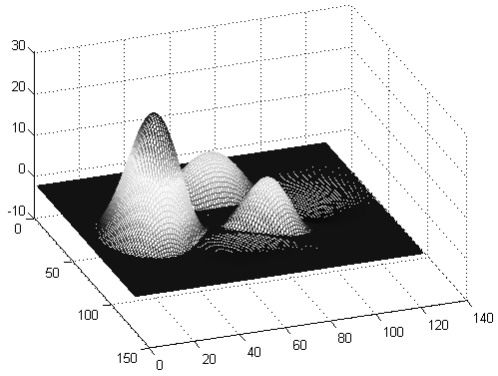

Fig. 6. Flattened phase surface of the scene

Iterative procedure for pixel height determination is applied to one pixel from the surface of interest. The initial value of Δz is 6 m. Eight iterations are made in order to obtain a scaling factor of value 7.5073. Multiplication of each point from flattened phase surface of the scene by a scaling factor yields a final reconstructed 3-D image, the topographic map of the scene of interest (Fig. 7).

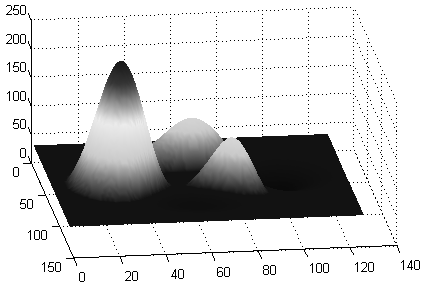

Fig. 7. Reconstructed 3-D image of the relief.

5. Conclusions

In the present work based on geometrical interpretation of Inverse Synthetic Aperture Radar (InSAR) scenario, main parameters, characteristics and operations over InSAR data have been defined. SAR interferogram and interferometric phase SAR equations have been derived and procedure of interferogram flattening has been given. The procedures of terrain motion evaluation and differential interferogram generation have been presented. Basic operations including rectification of the elevation map, co-registration, and coherence evaluation, and phase unwrapping have been discussed. Numerical experiment has been carried out to verify geometrical interpretation of the interferogam generation and main operation performance.

Acknowledgement

The work is supported by Project NATO CLG: ESP.EAP.CLG.983876, and Project ESA C1P-6051.

References

[1] Ferretti Al., Andrea Monti-Guarniery, Cl. Prari, F. Rocca, Didier Massonnet, “InSAR principles: guidelines for interferometry processing and interpretation: a practical approach, parts A,B,C”, ESA Publications, The Netherlands, 2007.

[2] Rocca F., Prati C., An Overview of SAR Interferometry, Dipartimento di Elettronica e Informazione (DEI) Politecnico di Milano (POLIMI), Piazza Leonardo da Vinci 32, 20133 Milano,Italy. rocca elet.polimi.it pratielet.polimi.it, http://www.elet.polimi.it

[3] H. Rott, T. Nagler. The contribution of radar interferometry to the assessment of landslide hazards Advances in Space Research 37 (2006) 710–719. www.elsevier.com/locate/asr

[4] Bamler, R., Adam, N., Davidson, G.W., et al. Noise-induced slope distortion in 2-D phase unwrapping by linear estimators with application to SAR interferometry. IEEE Trans. Geosci. Remote Sensing 36, 705–715, 1998.

[5] Goldstein R. M., H. Englehardt, B. Kamb and R. M. Frolich. Satellite radar interferometry for monitoring ice sheet motion: Application to an Antarctic Ice Stream, Science, vol. 262, no. 1, pp. 525-1,530, 1993.

[6] Lazarov, A.D, Ch. Minchev. Cluster Micro-satellite InSAR Model, SSW, Istanbul, 05-07 June, pp. 26-31, 2008

[7] Massonnet, D., M. Rossi, C. Carmona, F. Adragna, G. Peltzer, K. Feigl, and T. Rabaute, .The displacement field of the Landers earthquake mapped by radar interferometry, Nature, vol. 364, pp. 138-142, 1993.

[8] Reilinger, R.E., S. Ergintav, R. Bürgmann, S. McClusky at al. Coseismic and postseismic fault slip for the 17 August 1999, M=7.4, Izmit, Turkey earthquake, *Science*, *289*, 1519-1524. 2000

[9] Rott, H., Nagler, T., Rocca, F., et al. MUSCL – monitoring urban subsidence, cavities and landslides by remote sensing, EC Project EVG1-CT-1999-00008, Institute for Meteorology and Geophysics, University of Innsbruck, Austria, 2002.

[10] Desnos, Y.-L., Buc, C., Guijarro, J., et al. ASAR – Envisat's advanced synthetic aperture radar. ESA Bull. 102, 91–102, 2000.

[11] Gens, R. Two-dimensional phase unwrapping for radar interferometry: developments and new challenges. Int. J. Remote Sensing 24, 703–710, 2003.

[12] Siegel, A. Least squares unwrapping with iterative corrections, in: Proceedings of IGARSS_99, IEEE Cat. Nr. 99CH36293, pp. 2398–2400, 1999.

[13] Jose M. Bioucas-Dias1 and Goncalo Valadao, Phase Unwrapping via Graph Cuts, Instituto de Telecomunica_coes - Instituto Superior Tecnico, 2004.

[14] [http://cd-amr.fnal.gov/aas/poisson.pdf]

[15] [http://www.physics.buffalo.edu/phy516/Files/Topic4/mar6.pdf].